CHEMISTRY
A EUROPEAN JOURNAL

Structures and Magnetic Properties of Tetranuclear Nickel(II) Complexes with Unusual μ_3-1,1,3 Azido Bridges

Franc Meyer,*[a] Serhiy Demeshko,[a] Guido Leibeling,[a] Berthold Kersting,[b] Elisabeth Kaifer,[c] and Hans Pritzkow[c]

Abstract: Pyrazolate-based dinucleating ligands with thioether-containing chelate arms have been used for the synthesis of a family of novel tetranuclear nickel(II) complexes $[L_2Ni_4(N_3)_3(O_2CR)](ClO_4)_2$ that incorporate three azido bridges and one carboxylate (R = Me, Ph). Molecular structures have been elucidated by X-ray crystallography in four cases, revealing Ni_4 cores with a unique topology in which two of the azido ligands adopt an unusual μ_3-1,1,3 bridging mode. The compounds were further characterized by mass spectrometry, IR spectroscopy, and variable-temperature magnetic susceptibility measurements. Magnetic data analyses indicate a combination of significant intramolecular ferromagnetic and antiferromagnetic exchange interactions that give rise to an overall $S_T = 0$ ground state. The sign and the magnitude of the individual couplings have been rationalized in the framework of the common magnetostructural correlations for end-to-end and end-on azido linkages, suggesting that these correlations also remain valid for the respective fragments of multiply bridging μ_3-1,1,3 azido ligands.

Keywords: azide ligands · magnetic properties · molecular magnetism · nickel · tetranuclear complexes

Introduction

The last decade has seen extensive research devoted to the study of magnetic interactions between paramagnetic centers in exchange-coupled systems, which is fired by the growing interest in molecule-based magnetic materials.[1,2] One of the major incentives is to obtain nanoscale molecular magnets, and current activities focus on increasing the nuclearity of single-molecule clusters that have ground electronic states with a large spin[3] and enhancing the anisotropy of single-molecule type systems.[4] Nickel(II) is an attractive spin carrier for this purpose owing to its large single-ion zero-field splitting. A similarly active line of research is aimed at the synthesis and characterization of materials with molecular architectures extending to one, two, or three dimensions of space and exhibiting long-range magnetic ordering.[2,5,6]

For all these intertwined facets of research within the field of molecule-based magnetism, the flexidentate azido bridge plays a central role, since it may propagate different kinds of magnetic coupling depending on its mode of coordination.[7,8] A variety of molecular architectures for azido compounds of different dimensionality have been discovered,[8–13] in particular in nickel(II) chemistry.[8–12] Magnetostructural correlations for the two major binding modes of the azido ligand have emerged: μ-1,1 azido bridges (end-on,

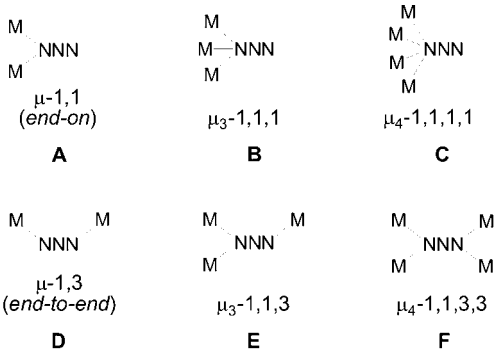

[a] Prof. Dr. F. Meyer, S. Demeshko, Dr. G. Leibeling
Institut für Anorganische Chemie
Georg-August-Universität Göttingen
Tammannstrasse 4, 37077 Göttingen (Germany)
Fax: (+49) 551-393-063
E-mail: franc.meyer@chemie.uni-goettingen.de

[b] Priv.-Doz. Dr. B. Kersting
Institut für Anorganische und Analytische Chemie
Universität Freiburg
Albertstrasse 21, 79104 Freiburg (Germany)

[c] Dr. E. Kaifer, Dr. H. Pritzkow
Anorganisch-Chemisches Institut, Universität Heidelberg
Im Neuenheimer Feld 270, 69120 Heidelberg (Germany)

DOI: 10.1002/chem.200400945

A) usually mediate ferromagnetic (F) coupling, whereas μ-1,3 azides (end-to-end, **D**) in most cases entail antiferromagnetic (AF) behavior. Few compounds with a triply bridging μ_3-1,1,1 mode **B** are known, mostly in $\{M_4(N_3)_4\}$ cubane clusters.[14] Examples for the μ_3-1,1,3 mode **E** (in which both AF and F exchange might occur) are very scarce and have only been reported for few 2D or 3D polymeric coordination networks[15] or most recently for some Ni_4 complexes.[11,12] In most cases, however, at least one of the M–N distances is very long, which limits their description as genuine μ_3-1,1,3 type azido ligands.[11,15] Novel μ_4-1,1,1,1 (**C**)[16] and μ_4-1,1,3,3 (**F**)[12,17] azide binding modes have only recently been reported. The paucity of complexes with the more unusual azide binding modes **C**, **E**, and **F** is highly unsatisfactory, since these types of azide bridges are particularly suited for the linking of several metal ions in high-nuclearity clusters and for the construction of 2D and 3D networks of paramagnetic metal centers. This is of major relevance, since magnetic ordering is essentially a three-dimensional property, and the design of a molecule-based magnet requires control of the molecular architecture along all three dimensions of space.[18] Hence, there is considerable interest in the exploration of these multiply bridging azide ligands in oligometallic clusters.

We recently communicated the first example of an unprecedented class of tetranuclear nickel(II) complexes that feature two different types of azide ligands, including genuine μ_3-1,1,3 azide bridges.[12] The present contribution gives a detailed report on the structural and spectroscopic characteristics of a series of these unique complexes and describes their magnetic properties.

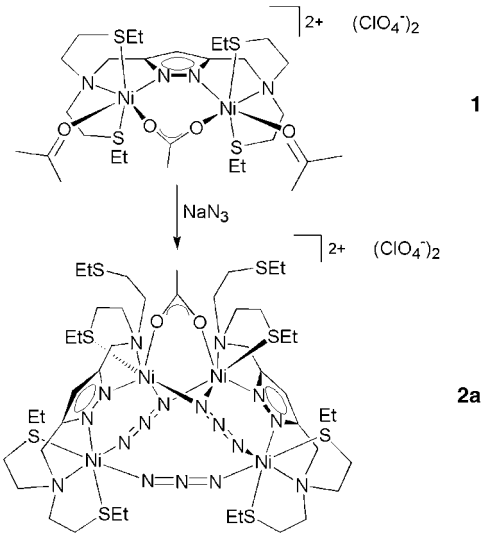

Scheme 1. Initial synthesis of **2a** from **1**.

Results and Discussion

Synthesis and structural characterization of the complexes: We have previously shown that pyrazolate-based bimetallic complexes with accessible coordination sites can serve as suitable building blocks for the assembly of polynuclear[11,17] aggregates or 1D extended-chain compounds with alternating bridges.[19,20] The first example (**2a**) of the new type **2** tetranuclear complexes was obtained serendipitously when we set out to assemble a 1D alternating chain from dinickel(II) building blocks $[L^1Ni_2(OAc)]^{2+}$, which was anticipated to occur upon replacement of the labile acetone ligands in **1**[21] by potentially bridging azide ions (Scheme 1). Unexpectedly however, treatment of a solution of **1** with NaN_3 led to a reshuffling of all azide and acetate ligands, giving the Ni_4 complex **2a** in good yield. Further experiments revealed that various type **2** complexes can be prepared directly from appropriate amounts of the respective components (Scheme 2). Pyrazolate-based ligands with different thioether substituents (L^1: R = Et; L^2: R = *i*Pr)[17,22] as well as different carboxylates have been used in order to evaluate the scope of these systems.

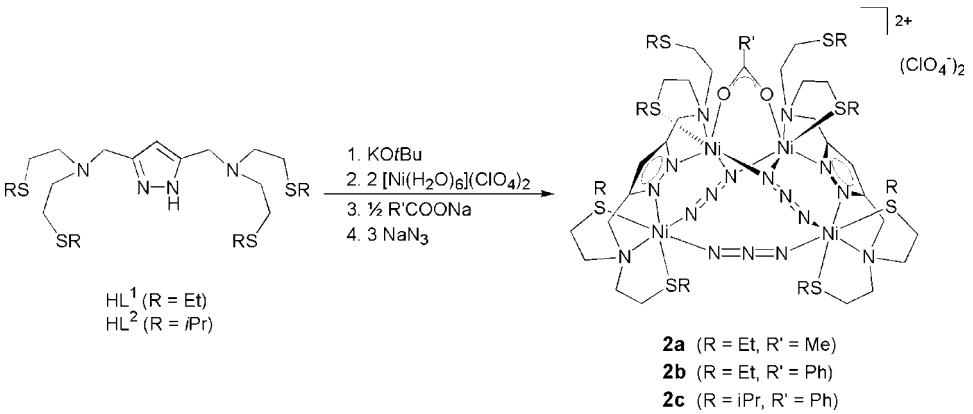

Scheme 2. Targeted synthesis of the complexes.

The tetranuclear nature of all these new complexes is indicated by FAB mass spectrometry. While the most intense signal corresponds to the species $[LNi_2(N_3)(O_2CR')]^+$, a signal for $[L_2Ni_4(N_3)_3(O_2CR')(ClO_4)]^+$ with the expected isotopic distribution pattern can be clearly detected in all cases. The FAB mass spectrum of **2b** is depicted in Figure 1 as an example.

A detailed picture of the molecular structures of **2a**–**2c** was obtained by X-ray crystallography. The overall structure of the cation and the unique central Ni_4 core of **2c** are depicted in Figure 2 as an example. Table 1 lists selected interatomic distances and bond angles for all three complexes, and a general numbering scheme is depicted in Figure 3. Complex **2a** could be crystallized with two different solvate

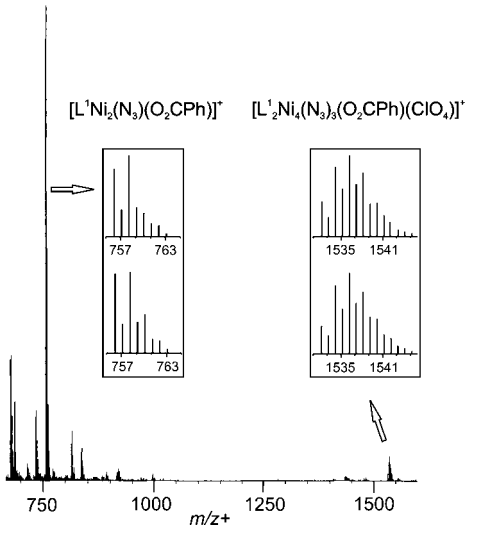

Figure 1. Positive-ion FAB-MS spectrum of **2b**; the inset shows the experimental (lower) and theoretical (upper) isotopic distribution pattern for dinuclear $[L^1Ni_2(N_3)(O_2CPh)]^+$ and tetranuclear $[L^1_2Ni_4(N_3)_3(O_2CPh)(ClO_4)]^+$ ions, respectively.

Table 1. Selected interatomic distances [Å] and angles [°] for complexes **2a**, **2b**, and **2c**.

	2a (from acetone)	**2a** (from CH_2Cl_2)	**2b**	**2c**
Ni1–N10//Ni3–N18	2.118(2)//2.143(2)	2.097(2)//2.152(3)	2.123(2)	2.135(2)
Ni1–N10a(N18)//Ni3–N10	2.150(2)//2.146(2)	2.160(2)//2.137(3)	2.133(2)	2.156(2)
Ni2–N12//Ni4–N16	2.115(3)//2.098(2)	2.099(3)//2.094(3)	2.094(2)	2.104(3)
Ni2–N13//Ni4–N15	2.058(3)//2.070(2)	2.067(3)//2.091(3)	2.089(2)	2.080(3)
N10–N11//N18–N17	1.194(3)//1.202(3)	1.191(3)//1.195(3)	1.196(3)	1.187(3)
N11–N12//N17–N16	1.168(3)//1.165(3)	1.163(3)//1.166(3)	1.165(3)	1.160(3)
N13–N14//N14–N15	1.172(3)//1.174(3)	1.172(3)//1.180(3)	1.176(2)	1.166(3)
Ni1–O60//Ni3–O61	2.018(2)//2.011(2)	2.032(2)//2.012(2)	2.034(2)	2.036 (2)
Ni1···Ni1a(Ni3)	3.151(1)	3.171(1)	3.175(1)	3.181(2)
Ni1···Ni2//Ni3···Ni4	4.479(1)//4.461(1)	4.444(1)//4.451(1)	4.466(1)	4.449(2)
Ni2···Ni2a(Ni4)	5.493(1)	5.498(1)	5.536(1)	5.589(2)
Ni1···Ni2a(Ni4)//Ni2···Ni1a(Ni3)	5.499(1)//5.419(1)	5.466(1)//5.427(1)	5.406(1)	5.494(2)
Ni1–N10–Ni1a(Ni3)//Ni1–N18–Ni3	95.3(1)//94.4(1)	97.0(1)//94.7(1)	96.5(1)	95.7(1)
Ni1-N10-N11//Ni3-N18-N17	120.2(2)//115.4(2)	118.8(2)//115.2(2)	118.8(2)	115.1(2)
Ni1-N10a(N18)-N11a(N17)//Ni3-N10-N11	124.0(2)//123.6(2)	122.4(2)//125.7(2)	123.8(2)	129.8(2)
Ni2-N12-N11//Ni4-N16-N17	116.9(2)//122.3(2)	117.9(2)//122.6(2)	118.6(2)	121.6(2)
Ni2-N13-N14//Ni4-N15-N14	128.1(2)//126.1(2)	128.6(2)//122.7(2)	125.6(2)	126.0(2)
Ni1-N10-N12-Ni2//Ni3-N18-N16-Ni4	14.1(2)//10.4(2)	20.7(2)//10.6(2)	17.3(2)	27.6(2)
Ni2-N12-N10-Ni1a(Ni3)//Ni4-N16-N18-Ni1	108.0(2)//105.5(2)	105.2(2)//104.3(2)	105.4(2)	95.6(2)
Ni2-N13-N13a(N15)-Ni2a(Ni4)	99.6(2)	104.1(2)	106.5(2)	116.9(2)

molecules (acetone or CH_2Cl_2), but the molecular structures for the two forms are almost identical.

The central core structures are quite similar for all three compounds investigated. The tetranuclear units consist of two LNi_2 fragments that are connected by three azido ligands and a single bridging carboxylate (in the crystal structures of **2b** and **2c** the two subunits are related by a C_2 axis). Two of the azido ligands are found in the rare μ_3-1,1,3 mode, whereas the third exhibits end-to-end binding between Ni2 and Ni2a (or Ni4, respectively). Ni–N_{azide} bond lengths for the μ_3-1,1,3 azides (2.094(2)–2.160(3) Å) are somewhat longer than for the μ-1,3 azide (2.058(3)–2.091(3) Å), but they are still in the usual range for azido ligands,[8,9] in contrast to most other systems with a μ_3-1,1,3 azide, which usually exhibit at least one very long M–N distance.[11,15] Whereas the end-to-end azido bridge is symmetric (d(N–N) = 1.172(2)–1.180(3) Å), the μ_3-1,1,3 bridges display markedly lengthened and shortened N–N bonds, respectively (d(N10–N11)/d(N17–N18) = 1.187(3)–1.202(3) Å versus d(N11–N12)/d(N16–N17) = 1.160(3)–1.168(3) Å). Further geometric parameters important with respect to the magnetic properties are the Ni–N–Ni angles for the end-on bridging part of the μ_3-1,1,3 azides, which lie in the narrow 94.4(1)–97.0(1)° range, as well as the Ni–N–N_{azide} angles (see Table 1). Dihedral Ni–NNN–Ni torsion angles along the μ_3-1,1,3 azide are in the 10.4–27.6° range (Ni1/Ni2 and Ni3/Ni4) and in the 95.6–108.0° range (Ni1/Ni2a(Ni4) and Ni2/Ni1a(Ni3)), while being 99.6–116.9° along the μ-1,3 bridge. Despite the more bulky isopropyl substituents of the ligand side arms in **2c**, metric parameters for the three complexes differ only slightly. Subtle differences may have some effect on magnetic properties of the Ni_4 cores, however, as is analyzed in more detail below. All nickel(II) ions in **2a**–**c** are six-coordinate, which leaves two of the thioether side arms of the pyrazolate ligands dangling (Scheme 2, Figure 2). The tetranickel entities are wrapped in their surrounding ligand matrices and are well separated from each other within the crystal lattice with closest intermolecular Ni···Ni contacts of 7.03 Å (**2a**·0.75 acetone), 7.18 Å (**2a**·1.95CH_2Cl_2), 7.63 Å (**2b**·2CH_2Cl_2), or 8.60 Å (**2c**).

Values for the $\nu_{as}(N_3)$ stretches observed in the IR spectra of the new complexes are collected in Table 2. All compounds feature a medium intensity band at about 2043 cm^{-1} and a very strong band at about 2083 cm^{-1} (with an additional shoulder at 2092 cm^{-1} in the case of **2a**). We tentatively assign the former to the μ-1,3 azide and the latter to the μ_3-1,1,3 bridges, in accordance with the trends in IR absorption observed for other pyrazolate-based dinuclear and tetranuclear nickel(II) complexes with azido ligands in various binding modes.[23,11,17]

Magnetic properties: Magnetic susceptibility measurements were carried out for powdered samples of complexes **2a**, **2b**, and **2c** in two different fields (2000 G and 5000 G), in a temperature range from 2.0 to 295 K. In no case was any significant field dependence of the magnetic data observed. Plots of the magnetic susceptibility χ_M versus T and of the product

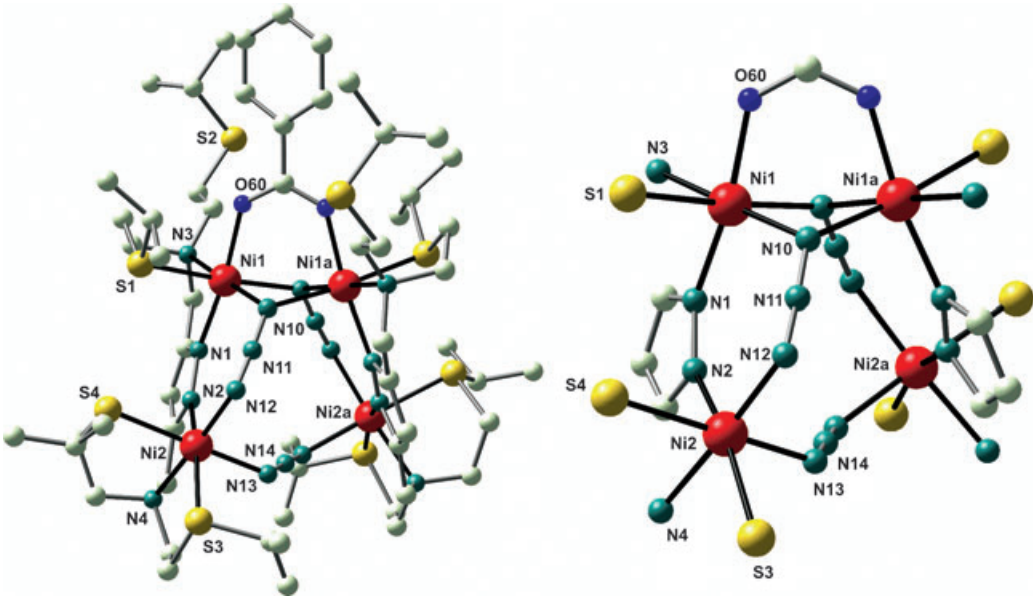

Figure 2. View of the molecular structure of the cation of **2c** (left) and of its central tetranuclear core (right). In the interest of clarity all hydrogen atoms have been omitted.

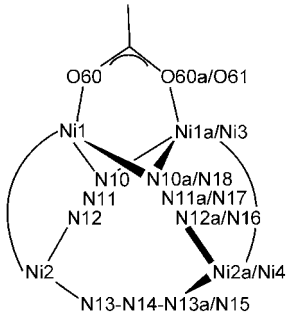

Figure 3. General numbering scheme for the central Ni_4 cores of **2a**–**2c**.

Table 2. Selected IR absorptions of complexes **2a**–**2c** [cm^{-1}].

complex	$\nu_{as}(N_3)$
2a	2042 (m), 2081 (vs), 2092 (sh)
2b	2043 (m), 2083 (vs)
2c	2043 (m), 2083 (vs)

$\chi_M T$ versus T for **2a**–**2c** measured at 2000 G are depicted in Figure 4.

For all complexes, $\chi_M T$ decreases rapidly when the temperature is lowered. At room temperature the $\chi_M T$ values are in the 3.35–3.62 $cm^3 K mol^{-1}$ range, that is, much lower than the value expected for four uncoupled nickel(II) centers (4.83 $cm^3 K mol^{-1}$ for $g = 2.2$). This is indicative of significant antiferromagnetic exchange coupling within the Ni_4 core, which is also evident from the broad maxima of the χ_M versus T curves that occur around 170–200 K. The $\chi_M T$ values tend towards zero at low temperatures, in accordance with dominant antiferromagnetic exchange and an $S_T = 0$ ground state. The rise of χ_M at very low temperatures is probably due to some residual paramagnetic impurity.

Considering the molecular topology of the complexes we can expect six magnetic exchange pathways according to Figure 5. As a simplifying approximation for magnetic data analysis, we assume twofold symmetry in all Ni_4 skeletons with $J_{1,2} = J_{3,4}$ and $J_{1,4} = J_{2,3}$. The overall coupling scheme thus comprises one *intra*dimer coupling by way of the pyrazolate and the *cis*-type end-to-end linkage of an μ_3-1,1,3 azide ($J_{1,2}/J_{3,4}$), but three *inter*dimer couplings: one through the carboxylate and the end-on linkages of the μ_3-1,1,3 azides ($J_{1,3}$), the second along the μ-1,3 azide bridge ($J_{2,4}$), and the third along the diagonals (*trans*-type end-to-end linkages of μ_3-1,1,3 azides) of the Ni_4-core ($J_{1,4}/J_{2,3}$). The experimental $\chi_M T$ data were analyzed by means of an appropriate model based on the isotropic Heisenberg–Dirac–van-Vleck (HDvV) exchange Hamiltonian in Equation (1), in which an additional term accounts for the Zeeman splitting and the g values are assumed to be identical for all positions.[24]

$$\begin{aligned} H = & -2J_{1,2}(\hat{S}_1\hat{S}_2 + \hat{S}_3\hat{S}_4) - 2J_{1,3}(\hat{S}_1\hat{S}_3) - 2J_{2,4}(\hat{S}_2\hat{S}_4) \\ & -2J_{1,4}(\hat{S}_1\hat{S}_4 + \hat{S}_2\hat{S}_3) + \sum g\mu_B B\hat{S}_{iz} \end{aligned} \quad (1)$$

Since the paramagnetic impurity and zero-field splitting effects were not taken into account, only data above 30 K (**2a**), 29 K (**2b**), and 25 K (**2c**) were included in the fitting procedure. The solid lines in Figure 4 represent the best fits to the experimental data for complexes **2a**–**2c**, which yield the parameters compiled in Table 3. Two dominant antiferromagnetic couplings and two ferromagnetic interactions are found for all complexes. Alternative models with, for example, three antiferromagnetic and one ferromagnetic inter-

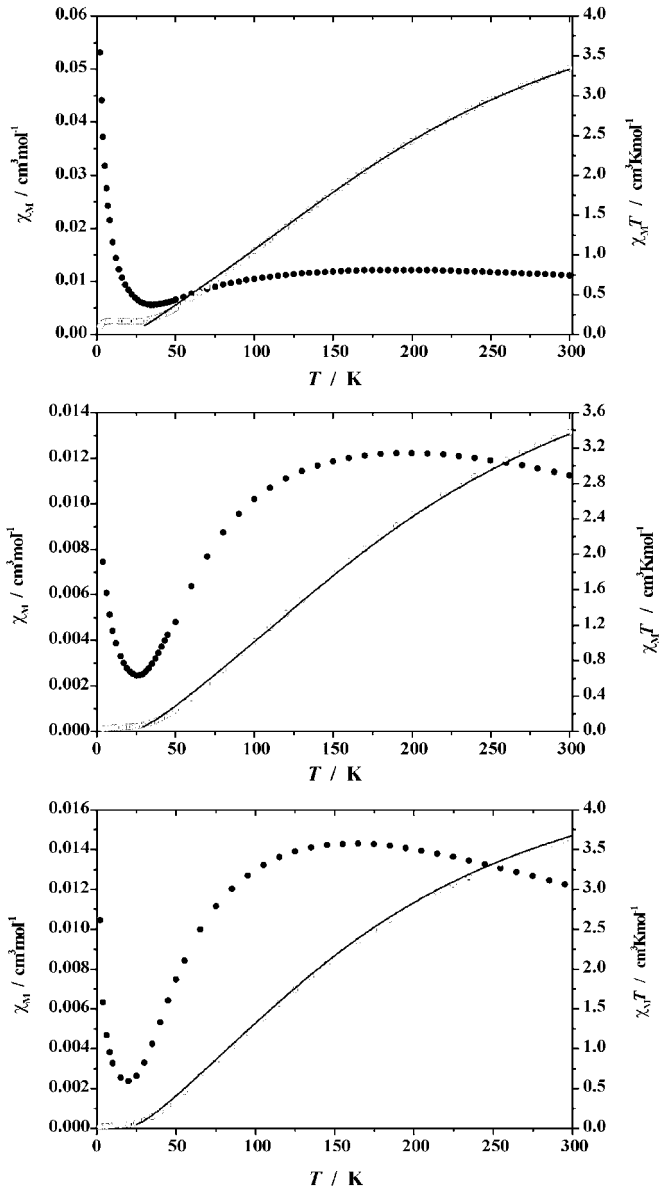

Figure 4. Plots of χ_M (solid circles) and $\chi_M T$ (open circles) versus temperature for **2a** (top), **2b** (middle), and **2c** (bottom) at 2000 G; the solid lines represent the calculated curve fits (see text).

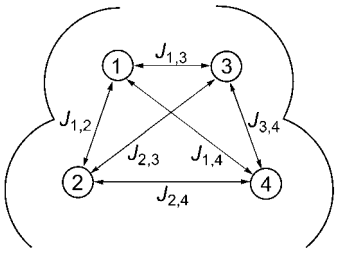

Figure 5. Magnetic coupling scheme for the complexes **2a**–**2c**.

actions clearly gave a worse fit. It should be noted that because of the symmetry of the Hamiltonian the individual interactions $J_{1,3}$, $J_{1,2}/J_{3,4}$, $J_{1,4}/J_{2,3}$, and $J_{2,4}$ are not unambiguously assigned to the topological J values in Figure 5, but assignment is based on rationalization in view of the known magnetostructural correlations for nickel(II) azido systems.[8]

Table 3. Best fit parameters for complexes **2a**–**2c**.

Complex	**2a**	**2b**	**2c**
$J_{1,3}$ [cm^{-1}]	+57	+25	+27
$J_{1,2}/J_{3,4}$ [cm^{-1}]	−51	−61	−53
$J_{2,3}/J_{1,4}$ [cm^{-1}]	−18	−12	−3
$J_{2,4}$ [cm^{-1}]	+6	+5	+6
g	2.29	2.38	2.30

To interpret the magnetic parameters determined for the various complexes, it appears reasonable to first consider separately the individual fragments of the tetranuclear framework. Ni1 and Ni2 (as well as Ni3 and Ni4) are spanned by the pyrazolate and by an end-to-end azide (as part of the central μ_3-1,1,3-azide), corresponding to $J_{1,2}$ and $J_{3,4}$ in Figure 5. While some exchange contribution from the pyrazolate is certainly present, it is likely that the azide provides the dominant exchange pathway within the pyrazolate-based bimetallic subunits.[21] Furthermore, there are two end-to-end *inter*dimer linkages through the μ_3-1,1,3-azide between the pyrazolate-based subunits (Ni1-NNN-Ni2a/Ni4 and Ni2-NNN-Ni1a/Ni3, corresponding to $J_{1,4}$ and $J_{2,3}$).

These different types of end-to-end azido connectivities established by the μ_3-1,1,3-azides are distinguished by drastically different Ni-NNN-Ni torsion angles, which are small (10.4–27.6°) in the *intra*dimer, but large (95.6–108.0°) in the *inter*dimer case. Finally, Ni2 and Ni2a (or Ni4, respectively) are also connected by an end-to-end azide, the coupling pathway denoted $J_{2,4}$.

A number of dinuclear nickel(II) complexes with only a single μ-1,3 azido bridge have been characterized magnetically.[25] For magnetostructural correlation, two geometric parameters are usually considered: the angles Ni-N-N and the dihedral angle ϕ along the azide ligand.[8,26] For a Ni-NNN-Ni torsion angle of $\phi = 180°$, the antiferromagnetic coupling is predicted to have a maximum at Ni-N-N angles around 108° and to decrease at larger angles. On the other hand, the maximum coupling for all Ni-N-N angles is expected for a torsion of 180° (or 0°). However, the effect of torsion should be less pronounced than the effect of bond angle. In the absence of any constraining ligand scaffold, Ni-N-N angles in dinuclear complexes or 1D extended systems with one μ-1,3 azido bridge tend to lie in the 115°–145° range with $\phi = 140°$–180°, resulting in J values in the −8 to −55 cm^{-1} range.[8,17] Particularly strong antiferromagnetic coupling of around −50 cm^{-1} has been observed for some 1D chain complexes with a *trans*-{Ni-(μ-1,3-N_3)-Ni} motif featuring acute Ni-N-N angles (120.9 or 115.6/116.8°, respectively) and a large ϕ (180° or 175.5°, respectively),[27] or in a dinickel(II) complex with extremely obtuse Ni-N-N angles of 109.9°.[8,28] In the case of complexes **2a**–**2c**, Ni-N-N angles for the *intra*dimer linkages involving the μ_3-1,1,3-azide are found in the narrow 115.6–121.7° range, and Ni1-NNN-Ni2 and Ni3-NNN-Ni4 torsion angles are not very far from zero

(10.4–27.6°). A large antiferromagnetic *intra*dimer coupling on the order of $-50\ cm^{-1}$ can thus be anticipated for **2a**–**2c**, in accordance with experimental findings for $J_{1,2}/J_{3,4}$ which are safely assigned to the *intra*dimer coupling. Among the series of three complexes **2a**–**2c**, *intra*dimer Ni-NNN-Ni torsion angles are largest for **2c** (27.6°) but somewhat smaller for **2a** and **2b** (10.4–20.7°). However, care should be taken when trying to relate the magnetic exchange constants to such minor differences of the metric parameters deduced from single crystal X-ray structures. First, values in Table 3 obtained from fits to the magnetic data can only be viewed as approximate values, since effects such zero-field splitting have not been taken into account. Second, magnetic measurements were performed on dried powered samples that in the case of **2a** and **2b** have lost the solvent of crystallization included in the crystal lattice. Although no major structural rearrangments are to be expected upon extrusion of the solvent molecules, subtle changes of bond angles cannot be fully excluded.

In contrast to the more common situation discussed above, the antiferromagnetic contribution for an end-to-end azido linkage is predicted to become negligible if the torsion ϕ along Ni-NNN-Ni approaches an orthogonal orientation close to 90°, or if the Ni-N-N bond angles exceed 155°.[8] A ferromagnetic interaction should result for this particular arrangement. Very few examples of such ferromagnetically coupled nickel(II) systems with μ-1,3 azido bridges have hitherto been discovered.[29,30,31] One is a dinuclear complex of a cryptate ligand that enforces unusual quasilinearity of the central Ni-NNN-Ni unit (Ni-N-N angles close to 165°),[30] whereas the others are 1D compounds[29] and a Ni_4 complex[31] that exhibit appropriate Ni-NNN-Ni torsion angles (ϕ = 110.4°, 106.8°, 75.7°, or 76.4°, respectively). In the latter cases, positive J values in the $+7$ to $+3\ cm^{-1}$ range have been attributed to quasiorthogonality between the magnetic metal orbitals and the relevant azide p orbitals, which causes minimal overlap integrals through the bridge and hence a vanishing antiferromagnetic exchange contribution.[29] *Inter*dimer torsion angles of the diagonal end-to-end Ni1-NNN-Ni2a/Ni4 and Ni2-NNN-Ni1a/Ni3 linkages involving the μ_3-1,1,3-azide are found in the 104.3–108.0° range for **2a** and **2b**, and the situation is even more close to orthogonality for **2c** (ϕ = 95.6°). Accordingly, antiferromagnetic coupling $J_{2,3}/J_{1,4}$ should be much less pronounced than the *intra*dimer coupling $J_{1,2}/J_{3,4}$, as is observed experimentally. The *inter*dimer interaction for $J_{2,3}/J_{1,4}$ is still antiferromagnetic, however, which is presumably due to the Ni-N-N angles being significantly smaller than 155° (mean value for **2a**–**2c**: 120.7°). On the other hand, the μ-1,3 azido bridge connecting Ni2 and Ni2a/Ni4 exhibits somewhat larger Ni-N-N angles (mean value 126.2°) in conjunction with appropriate Ni-NNN-Ni torsion (ϕ = 99.6–116.9°) to apparently reach the ferromagnetic regime, and $J_{2,4}$ is found to be around $+5\ cm^{-1}$ for **2a**–**2c**. Interestingly, the combination of strong ferromagnetic coupling propagated through the {Ni(μ-1,1-N_3)$_2$Ni} linkage between Ni1 and Ni3/Ni1a ($J_{1,3}$, see below) and dominant antiferromagnetic *intra*dimer exchange ($J_{1,2}$,$J_{3,4}$) should lead to some degree of frustration in the Ni_4 array if the interdimer coupling $J_{2,4}$ were not of the ferromagnetic type.

Dinuclear nickel(II) complexes with two end-on azido bridges and a {Ni(μ-1,1-N_3)$_2$Ni} central core generally feature Ni–N–Ni angles θ in the narrow 101–105° range and J values between $+13$ and $+37\ cm^{-1}$.[8,9] DFT calculations suggested a clear correlation between the exchange coupling and θ, with the interaction predicted to be ferromagnetic for all the range of θ angles explored.[32] For the {Ni(μ-1,1-N_3)$_2$Ni} core, a maximum is expected at $\theta \approx 104°$. Ferromagnetic exchange has even been reported for a μ-1,1 azido-bridged nickel(II) dimer with a very large θ value of 129.3°, corroborating that a μ-1,1 azido group may be considered an almost universal ferromagnetic coupler.[33] On the other hand, the out-of-plane displacement of the azide should only have a minor influence. Ni1-N10-Ni3/Ni1a and Ni1-N18-Ni3 bond angles involving the μ_3-1,1,3-azide in complexes **2a**–**2c** are quite acute in the narrow range 94.4–97.0°. Significant ferromagnetic interaction between Ni1 and Ni1a/Ni3 can thus be anticipated, in accordance with the values obtained for $J_{1,3}$ (Table 3). The main structural difference between **2a** ($J_{1,3} = +57\ cm^{-1}$) and **2b**, **2c** ($J_{1,3} = +25$ and $+27\ cm^{-1}$, respectively) is the presence of an acetate versus benzoate bridge spanning Ni1 and Ni1a/Ni3. While $J_{1,3}$ is clearly dominated by the ferromagnetic contribution arising from the {Ni(μ-1,1-N_3)$_2$Ni} motif, it might be speculated that the benzoate imparts a more significant antiferromagnetic contribution than the acetate, reducing $J_{1,3}$ in the case of **2b** and **2c**.

Conclusion

A series of tetranuclear nickel(II) azido complexes composed of pyrazolate-based bimetallic building blocks has been characterized structurally and magnetically. The Ni_4 cores feature a unique topology and incorporate two azido ligands in the unusual μ_3-1,1,3 bridging mode, in addition to a μ-1,3 azide. Two types of ferromagnetic and two types of antiferromagnetic exchange interactions propagated by the different azido bridges have been identified, the combination of which gives rise to an overall $S_T = 0$ ground state. Magnetic couplings have been rationalized in the framework of the common magnetostructural correlations for end-to-end and end-on azido linkages,[8] suggesting that these correlations also remain valid for the respective fragments of multiply bridging μ_3-1,1,3 azido ligands. The results are in accordance with similar conclusions recently reached for μ_4-1,1,3,3 azides.[17] Future work will probe the possibilities of using such multiply bridging azides—which allow linkage of several metal ions—as efficient magnetic exchange mediators in high-nuclearity clusters and extended coordination networks.

Experimental Section

General: Commercial grade chemicals were used for synthetic procedures, and solvents were dried by established processes. Ligands HL^1 and HL^2 were synthesized according to the reported method.[17,22] Microanalyses were performed by the Analytisches Labor des Instituts für Anorganische Chemie der Universität Göttingen. IR spectra were recorded as KBr pellets on a Digilab Excalibur. Mass spectra were obtained with a Finnigan MAT 95 (FAB-MS). The susceptibility measurements were carried out with a Quantum-Design MPMS-5S SQUID magnetometer in the range from 295 to 2 K. The powdered samples were contained in a gel bucket and fixed in a nonmagnetic sample holder. Each raw data file for the measured magnetic moment was corrected for the diamagnetic contributions of the sample holder and the gel bucket. The molar susceptibilities were corrected for diamagnetism by using the Pascal constants and the increment method according to Haberditzl.[34]

Caution! Although no problems were encountered in this work, transition-metal perchlorate and azide complexes are potentially explosive and should be handled with proper precautions.

General synthesis of the complexes: For **2a**, a solution of HL^1 (256 mg, 0.535 mmol) in methanol (30 mL) was treated with KO*t*Bu (1 equiv, 63 mg, 0.535 mmol), $Ni(ClO_4)_2{\cdot}6H_2O$ (1.75 equiv, 294 mg, 0.803 mmol), and $Ni(O_2CMe)_2{\cdot}4H_2O$ (0.25 equiv, 33 mg, 0.134 mmol). For **2b** and **2c**, a solution of HL^1 (256 mg, 0.535 mmol) or HL^2 (286 mg, 0.535 mmol), respectively, in methanol (30 mL) was treated with KO*t*Bu (1 equiv, 63 mg, 0.535 mmol), $Ni(ClO_4)_2{\cdot}6H_2O$ (2 equiv, 391 mg, 1.07 mmol), and NaO_2CPh (0.5 equiv, 39 mg, 0.268 mmol). After stirring the mixture for 2 h at room temperature the solution was evaporated to dryness and the residue was taken up in acetone (25 mL). NaN_3 (52 mg, 0.803 mmol) was added and the reaction mixture stirred for a further 24 h. The precipitate was separated by filtration and the resulting green solution was layered with light petroleum ether (boiling range 40–60 °C, 75 mL) to obtain green crystals of the product **2a** (187 mg, 43 %), **2b** (202 mg, 46 %), or **2c** (270 mg, 58 %). In the case of **2a**, some crystalline material was redissolved in CH_2Cl_2 and crystals could be obtained from that solvent after layering the solution with light petroleum.

Analytical data for 2a: (crystals from acetone) IR (KBr): $\tilde{\nu}$ = 2092 (sh), 2081 (vs, $\nu(N_3^-)$), 2042 (m, $\nu(N_3^-)$), 1707 (w, $\nu(C{=}O)_{acetone}$), 1584 (m, $\nu(C{=}O)_{acetate}$), 1090 cm^{-1} (vs, $\nu(ClO_4^-)$); MS (FAB+, nibeol): *m*/*z* (%): 1474 (6) $[(L^1)_2Ni_4(N_3)_3(O_2CMe)(ClO_4)]^+$, 753 (12) $[L^1Ni_2(O_2CMe)(ClO_4)]^+$, 736 (25) $[L^1Ni_2(N_3)(ClO_4)]^+$, 696 (100) $[L^1Ni_2(N_3)(O_2CMe)]^+$, 677 (35), $[L^1Ni_2(N_3)_2]^+$; elemental analysis calcd (%) for $C_{44}H_{85}Cl_2Ni_4N_{17}O_{10}S_8{\cdot}0.75\,C_3H_6O$ (1618.02): C 34.33, H 5.47, N 14.72; found: C 34.20, H 5.58, N 14.87.

Analytical data for 2a: (crystals from CH_2Cl_2) elemental analysis calcd (%) for $C_{44}H_{85}Cl_2Ni_4N_{17}O_{10}S_8{\cdot}0.5\,CH_2Cl_2$ (1616.93): C 33.06, H 5.36, N 14.73, Cl 6.58; found: C 33.21, H 5.15, N 14.08, Cl 6.06.

Analytical data for 2b: IR (KBr): $\tilde{\nu}$ = 2083 (vs, $\nu(N_3^-)$), 2043 (m, $\nu(N_3^-)$), 1598 (m), 1563 (m, $\nu(C{=}O)_{benzoate}$), 1097 cm^{-1} (vs, $\nu(ClO_4)$); MS (FAB+, nibeol): *m*/*z* (%): 1536 (7) $[(L^1)_2Ni_4(N_3)_3(O_2CPh)(ClO_4)]^+$, 758 (100) $[L^1Ni_2(N_3)(O_2CPh)]^+$, 677 (33) $[L^1Ni_2(N_3)_2]^+$, 635 (18) $[L^1Ni_2(N_3)]^+$; elemental analysis calcd (%) for $C_{49}H_{87}Cl_2Ni_4N_{17}O_{10}S_8$ (1636.53): C 35.96, H 5.36, N 14.55; found: C 36.12, H 5.19, N 14.59.

Analytical data for 2c: IR (KBr): $\tilde{\nu}$ = 2083 (vs, $\nu(N_3^-)$), 2043 (m, $\nu(N_3^-)$), 1600 (m), 1564 (m, $\nu(C{=}O)_{benzoate}$), 1098 cm^{-1} (vs, $\nu(ClO_4)$); MS (FAB+, nibeol): *m*/*z* (%): 1648 (8) $[(L^2)_2Ni_4(N_3)_3(O_2CPh)(ClO_4)]^+$, 814 (100) $[L^2Ni_2(N_3)(O_2CPh)]^+$, 735 (24) $[L^2Ni_2(N_3)_2]^+$, 693 (16) $[L^2Ni_2(N_3)]^+$; elemental analysis calcd (%) for $C_{57}H_{103}Cl_2Ni_4N_{17}O_{10}S_8$ (1748.74): C 39.15, H 5.94, N 13.62; found: C 39.27, H 6.02, N 13.70.

X-ray crystallographic study: Data collection for **2a** and **2b** was carried out on a Nonius Kappa CCD diffractometer at 200 K, for **2c** on a Bruker AXS CCD diffractometer at 297 K using graphite-monochromated $Mo_{K\alpha}$ radiation (λ = 0.71073 Å). Structures were solved by direct methods (SHELXS-97) and refined by full-matrix least-squares techniques based on F^2 (SHELXL-97).[35] Atomic coordinates and thermal parameters of the nonhydrogen atoms were refined in fully anisotropic models. Hydrogen atoms were included by using the riding model with U_{iso} tied to U_{iso} of the parent atoms. Crystal data and refinement details are listed in Table 4. CCDC-149456 (**2a**·0.75 acetone), CCDC-244075 (**2a**·1.95 CH_2Cl_2), CCDC-149457 (**2b**), and CCDC-244076 (**2c**) contains the supplementary crystallographic data for this paper. These data can be obtained free of charge from The Cambridge Crystallographic Data Centre via www.ccdc.cam.ac.uk/data_request/cif.

Table 4. Crystal data and refinement details for complexes **2a**, **2b**, and **2c**.

	2a (from acetone)	**2a** (from CH_2Cl_2)	**2b**	**2c**
formula	$C_{44}H_{85}Cl_2Ni_4N_{17}O_{10}S_8{\cdot}0.75\,C_3H_6O$	$C_{44}H_{85}Cl_2Ni_4N_{17}O_{10}S_8{\cdot}1.95\,CH_2Cl_2$	$C_{49}H_{87}Cl_2Ni_4N_{17}O_{10}S_8{\cdot}2\,CH_2Cl_2$	$C_{57}H_{103}Cl_2Ni_4N_{17}O_{10}S_8$
M_r [g mol^{-1}]	1618.02	1740.12	1806.39	1748.74
crystal size [mm]	0.30×0.20×0.20	0.40×0.30×0.30	0.50×0.35×0.30	0.40×0.10×0.10
crystal system	monoclinic	monoclinic	monoclinic	monoclinic
space group	$P2_1/c$	$P2_1/c$	$I2/a$	$C2/c$
a [Å]	21.140(4)	20.951(4)	21.654(4)	27.9271(11)
b [Å]	16.348(3)	15.571(3)	15.490(3)	15.9843(6)
c [Å]	22.316(5)	22.906(5)	22.828(5)	22.4234(9)
α [°]	90	90	90	90
β [°]	113.59(3)	103.02(3)	104.61(3)	126.286 (1)
γ [°]	90	90	90	90
volume [Å^3]	7068(2)	7280(3)	7410	8068.5(5)
ρ_{calcd} [g cm^{-3}]	1.521	1.588	1.619	1.440
Z	4	4	4	4
F(000)	3384	3616	3752	3672
temperature [K]	200	200	200	297(2)
hkl range	−28 to 28, −22 to 22, −30 to 30	−27 to 27, −20 to 20, −29 to 29	−28 to 28, −20 to 18, −29 to 29	−37 to 30, 0 to 21, 0 to 29
2θ range [°]	3.4 to 58.0	3.3 to 55.2	3.7 to 55.0	3.1 to 56.6
measd reflns	43065	33488	14906	42837
unique reflns	18801 [R(int) = 0.0446]	16737 [R(int) = 0.0396]	8461 [R(int) = 0.0348]	10022 [R(int) = 0.0470]
obsd reflns [$I>2\sigma(I)$]12291	11734	6505	6876	
refinined params	887	902	442	580
resid electron density [e Å^{-3}]	0.970 and −0.670	0.728 and −0.562	0.911 and −0.749	0.616 and −0.438
*R*1 [$I>2\sigma(I)$]0.0423	0.0376	0.0406	0.0404	
*wR*2 (refinement on F^2)	0.1167	0.0956	0.1076	0.1177
goodness-of-fit	1.043	1.023	1.051	1.050

Acknowledgements

Financial support by the DFG (priority program 1137 "Molecular Magnetism") and the Fonds der Chemischen Industrie is gratefully acknowledged.

[1] a) O. Kahn, *Angew. Chem.* **1985**, *97*, 837–853; *Angew. Chem. Int. Ed. Engl.* **1985**, *24*, 834–850; b) O. Kahn, *Molecular Magnetism*, VCH, Weinheim, **1993**; c) J. S. Miller, A. J. Epstein, *Angew. Chem.* **1994**, *106*, 399–432; *Angew. Chem. Int. Ed. Engl.* **1994**, *33*, 385–388; d) *Molecule-Based Magnetic Materials* (Eds.: M. M. Turnbull, T. Sugimoto, L. K. Thompson), ACS Symposium Series 644, ACS, Washington, **1996**.

[2] *Magnetism: Molecules to Materials* (Eds.: J. S. Miller, M. Drillon), Wiley-VCH, Weinheim, **2001**.

[3] a) R. Sessoli, H.-L. Tsai, A. R. Schake, S. Wang, J. B. Vincent, K. Folting, D. Gatteschi, G. Christou, D. N. Hendrickson, *J. Am. Chem. Soc.* **1993**, *115*, 1804–1816; b) A. K. Powell, S. L. Heath, D. Gatteschi, L. Pardi, R. Sessoli, G. Spina, F. Del Giallo, F. Pieralli, *J. Am. Chem. Soc.* **1995**, *117*, 2491–2502; c) A. Müller, F. Peters, M. T. Pope, D. Gatteschi, *Chem. Rev.* **1998**, *98*, 239–271; d) D. Gatteschi, R. Sessoli, A. Cornia, *Chem. Commun.* **2000**, 725–732; e) J. Larionova, M. Gross, M. Pilkington, H. Andres, H. Stoeckli-Evans, H. U. Güdel, S. Decurtins, *Angew. Chem.* **2000**, *112*, 1667–1672; *Angew. Chem. Int. Ed.* **2000**, *39*, 1605–1609.

[4] a) O. Kahn, *Spec. Publ. 252 (Metal-Organic and Organic Molecular Magnets)*, Royal Society of Chemistry, **2000**, 150–168; b) O. Kahn, J. Larionova, L. Ouahab, *Chem. Commun.* **1999**, 945–952; c) A. Caneschi, D. Gatteschi, C. Sangregorio, R. Sessoli, L. Sorace, A. Cornia, M. A. Novak, C. Paulsen, W. Wernsdorfer, *J. Magn. Magn. Mater.* **1999**, *200*, 182–201.

[5] *Organic and Inorganic Low Dimensional Crystalline Material* (Eds.: P. Delhaes, M. Drillon), NATO ASI Series, Series B: Physics Vol. *168*, Plenum, New York, **1987**.

[6] See for example: a) S. Ferlay, T. Mallah, R. Ouahès, P. Veillet, M. Verdaguer, *Nature* **1995**, *378*, 701–703; b) K. Inoue, T. Hayamizu, H. Iwamura, D. Hashizume, Y. Ohashi, *J. Am. Chem. Soc.* **1996**, *118*, 1803–1804; c) S. R. Batten, K. S. Murray, *Coord. Chem. Rev.* **2003**, *246*, 103–130.

[7] a) M.-F. Charlot, O. Kahn, M. Chaillet, C. Larrieu, *J. Am. Chem. Soc.* **1986**, *108*, 2574–2581; b) R. Cortés, L. Lezama, F. A. Mautner, T. Rojo, in ref. [1 d], p 187; c) P. Chauduri, T. Weyhermüller, E. Bill, K. Wieghardt, *Inorg. Chim. Acta* **1996**, *252*, 195–202; d) L. K. Thompson, S. S. Tandon, *Comments Inorg. Chem.* **1996**, *18*, 125–144.

[8] J. Ribas, A. Escuer, M. Monfort, R. Vicente, R. Cortés, L. Lezama, T. Rojo, *Coord. Chem. Rev.* **1999**, *193–195*, 1027–1068; and references therein.

[9] F. Meyer, H. Kozlowski in *Comprehensive Coordination Chemistry II*, *Vol. 6* (Eds.: J. A. McCleverty, T. J. Meyer), Pergamon, **2004**, 247–554.

[10] Examples for Ni_4 complexes: a) J. Ribas, M. Monfort, R. Costa, X. Solans, *Inorg. Chem.* **1993**, *32*, 695–699; b) Z. E. Serna, L. Lezama, M. K. Urtiaga, M. I. Arriortua, M. G. Barandika, R. Cortés, T. Rojo, *Angew. Chem.* **2000**, *112*, 352–355; *Angew. Chem. Int. Ed.* **2000**, *39*, 344–347; c) Z. E. Serna, M. G. Barandika, R. Cortés, M. K. Urtiaga, G. E. Barberis, T. Rojo, *J. Chem. Soc. Dalton Trans.* **2000**, 29–34.

[11] G. Leibeling, S Demeshko, B. Bauer-Siebenlist, F. Meyer, H. Pritzkow, *Eur. J. Inorg. Chem.* **2004**, 2413–2420.

[12] F. Meyer, P. Kircher, H. Pritzkow, *Chem. Commun.* **2003**, 774–775.

[13] See for example: a) A. Escuer, R. Vicente, M. S. El Fallah, M. A. S. Goher, F. A. Mautner, *Inorg. Chem.* **1998**, *37*, 4466–4469; b) M. A. M. Abu-Youssef, A. Escuer, M. A. S. Goher, F. A. Mautner, G. J. Reiß, R. Vicente, *Angew. Chem.* **2000**, *112*, 1681–1683; *Angew. Chem. Int. Ed.* **2000**, *39*, 1624–1626; c) H.-Y. Shen, W.-M. Bu, E.-Q. Gao, D.-Z. Liao, Z.-H. Jiang, S.-P. Yan, G.-L. Wang, *Inorg. Chem.* **2000**, *39*, 396–400; d) M. A. Abu-Youssef, M. Drillon, A. Escuer, M. A. S. Goher, F. A. Mautner, R. Vicente, *Inorg. Chem.* **2000**, *39*, 5022–5027.

[14] a) M. A. Halcrow, J. C. Huffman, G. Christou, *Angew. Chem.* **1995**, *107*, 971–973; *Angew. Chem. Int. Ed. Engl.* **1995**, *34*, 889–891; b) M. A. Halcrow, J.-S. Sun, J. C. Huffman, G. Christou, *Inorg. Chem.* **1995**, *34*, 4167–4177; c) M. W. Wemple, D. M. Adams, K. S. Hagen, K. Folting, D. N. Hendrickson, G. Christou, *J. Chem. Soc. Chem. Commun.* **1995**, 1591–1593; d) D. Ma, S. Hikichi, M. Akita, Y. Moro-oka, *J. Chem. Soc. Dalton Trans.* **2000**, 1123–1134; e) M. A. S. Goher, J. Cano, Y. Journaux, M. A. M. Abu-Youssef, F. A. Mautner, A. Escuer, R. Vicente, *Chem. Eur. J.* **2000**, *6*, 778–784.

[15] a) M. Monfort, J. Ribas, X. Solans, *J. Chem. Soc. Chem. Commun.* **1993**, 350–351; b) J. Ribas, M. Monfort, X. Solans, M. Drillon, *Inorg. Chem.* **1994**, *33*, 742–745; c) I. Agrell, *Acta Chem. Scand.* **1967**, *21*, 2647–2658; d) M. A. S. Goher, A. Escuer, M. A. M. Abu-Youssef, F. A. Mautner, *Polyhedron* **1998**, *17*, 4265–4273; e) T. K. Maji, P. S. Mukherjee, S. Koner, G. Mostafa, J.-P. Tuchagues, N. R. Chaudhuri, *Inorg. Chim. Acta* **2001**, *314*, 111–116.

[16] a) G. S. Papaefstathiou, S. P. Perlepes, A. Escuer, R. Vicente, M. Font-Bardia, X. Solans, *Angew. Chem.* **2001**, *113*, 908–910; *Angew. Chem. Int. Ed.* **2001**, *40*, 884–886; b) G. S. Papaefstathiou, A. Escuer, R. Vicente, M. Font-Bardia, X. Solans, S. P. Perlepes, *Chem. Commun.* **2001**, 2414–2415; c) A. K. Boudalis, B. Donnadieu, V. Nastopoulos, J. M. Clemente-Juan, A. Mari, Y. Sanakis, J.-P. Tuchagues, S. P. Perlepes, *Angew. Chem.* **2004**, *116*, 2316–2320; *Angew. Chem. Int. Ed.* **2004**, *43*, 2266–2270.

[17] S. Demeshko, G. Leibeling, W. Maringgele, F. Meyer, C. Mennerich, H.-H. Klauss, H. Pritzkow, *Inorg. Chem.* in press.

[18] a) O. Kahn, *Acc. Chem. Res.* **2000**, *33*, 647–657; b) M. Pilkington, S. Decurtins, *Chimia* **2000**, *54*, 593–601.

[19] F. Meyer, U. Ruschewitz, P. Schober, B. Antelmann, L. Zsolnai, *J. Chem. Soc. Dalton Trans.* **1998**, 1181–1186.

[20] F. Meyer, H. Pritzkow, *Inorg. Chem. Commun.* **2001**, *4*, 305–307.

[21] M. Konrad, F. Meyer, A. Jacobi, P. Kircher, P. Rutsch, L. Zsolnai, *Inorg. Chem.* **1999**, *38*, 4559–4566.

[22] M. Konrad, F. Meyer, K. Heinze, L. Zsolnai, *J. Chem. Soc. Dalton Trans.* **1998**, 199–205.

[23] I. Agrell, *Acta Chem. Scand.* **1971**, *25*, 2965–2974.

[24] The program used here is a modification of the program described in ref. [31] The Hamiltonian matrix was diagonalized numerically to obtain the energies of the spin states, which on substitution into the van Vleck formula gave the theoretical values for the magnetic susceptibility. A least-squares program then compared calculated and observed susceptibility curves and changed the parameters to get the best fit.

[25] a) C. G. Pierpont, D. N. Hendrickson, D. M. Duggan, F. Wagner, E. K. Barefield, *Inorg. Chem.* **1975**, *14*, 604–610; b) F. Wagner, M. T. Mocella, M. J. D'Aniello Jr., A. H. J. Wang, E. K. Barefield, *J. Am. Chem. Soc.* **1974**, *96*, 2625–2627; c) G. A. McLachlan, G. D. Fallon, R. L. Martin, B. Moubaraki, K. S. Murray, L. Spiccia, *Inorg. Chem.* **1994**, *33*, 4663–4668; d) L. Fabbrizzi, P. Pallavicini, L. Parodi, A. Perotti, N. Sardone, A. Taglietti, *Inorg. Chim. Acta* **1996**, *244*, 7–9; e) A. Escuer, C. J. Harding, Y. Dussart, J. Nelson, V. McKee, R. Vicente, *J. Chem. Soc. Dalton Trans.* **1999**, 223–228; f) Z.-H. Zhang, X.-H. Bu, Z.-H. Ma, W.-M. Bu, Y. Tang, Q.-H. Zhao, *Polyhedron* **2000**, *19*, 1559–1566.

[26] F. F. de Biani, E. Ruiz, J. Cano, J. J. Novoa, S. Alvarez, *Inorg. Chem.* **2000**, *39*, 3221–3229.

[27] R. Vicente, A. Escuer, J. Ribas, M. S. El Fallah, X. Solans, M. Font-Bardia, *Inorg. Chem.* **1995**, *34*, 1278–1281.

[28] J. Hausmann, M. H. Klingele, V. Lozan, G. Steinfeld, D. Siebert, Y. Journaux, J. J. Girerd, B. Kersting, *Chem. Eur. J.* **2004**, *10*, 1716–1728.

[29] a) C. S. Hong, Y. Do, *Angew. Chem.* **1999**, *111*, 153–155; *Angew. Chem. Int. Ed.* **1999**, *38*, 193–195; b) M. Monfort, I. Resino, J. Ribas, H. Stoeckli-Evans, *Angew. Chem.* **2000**, *112*, 197–199; *Angew. Chem. Int. Ed.* **2000**, *39*, 191–193; c) C. S. Hong, J. E. Koo; S.-K. Son, Y. S. Lee, Y.-S. Kim, Y. Do, *Chem. Eur. J.* **2001**, *7*, 4243–

4252; d) P. S. Mukherjee, S. Dalai, E. Zangrando, F. Lloret, N. R. Chaudhuri, *Chem. Commun.* **2001**, 1444–1445.
[30] A. Escuer, C. J. Harding, Y. Dussart, J. Nelson, V. McKee, R. Vicente, *J. Chem. Soc. Dalton Trans.* **1999**, 223–228.
[31] B. Kersting, G. Steinfeld, D. Siebert, *Chem. Eur. J.* **2001**, *7*, 4253–4258.
[32] E. Ruiz, J. Cano, S. Alvarez, P. Alemany, *J. Am. Chem. Soc.* **1998**, *120*, 11122–11129.
[33] P. Mialane, A. Dolbecq, E. Rivière, J. Marrot, F. Sécheresse, *Angew. Chem.* **2004**, *116*, 2324–2327; *Angew. Chem. Int. Ed.* **2004**, *43*, 2274–2277.
[34] a) W. Haberditzl, *Angew. Chem.* **1966**, *78*, 277–288; *Angew. Chem. Int. Ed. Engl.* **1966**, *5*, 288–298; b) W. Haberditzl, *Magnetochemie*, Akademie-Verlag, Berlin, **1968**.
[35] G. M. Sheldrick, SHELXS-97, Program for Crystal Structure Solution, Universität Göttingen, **1997**; G. M. Sheldrick, SHELXL-97, Program for Crystal Structure Refinement, Universität Göttingen, **1997**.

Received: September 15, 2004
Published online: January 24, 2005